Development of a 3D ultrafast laser written near-infrared spectro-interferometer

G. Martin, G. Zhang, M. Bonduelle, R. Allaw, M. Callejo, A. Morand, A. Rodenas, G. Cheng, R. Stoian, C. D'amico

Development of a 3D ultrafast laser written near-infrared spectro-interferometer

G. MARTIN, [1,*] G. ZHANG,[2] M. BONDUELLE,[1] R. ALLAW,[1] M. CALLEJO,[3] A. MORAND,[3] A. RODENAS,[4,5] G. CHENG,[2] R. STOIAN,[6] AND C. D'AMICO,[6]

[1] *Univ. Grenoble Alpes/CNRS, IPAG, F-38000 Grenoble, France*
[2] *School of Artificial Intelligence, Optics and Electronics (iOPEN), Northwestern Polytechnical University, Xi'an, Shaanxi 710072, China*
[3] *Univ. Grenoble Alpes/CNRS/ Grenoble INP, IMEP-LAHC, F-38000 Grenoble, France*
[4] *Departamento de Física, Universidad de La Laguna (ULL), Apdo. 456, E-38200 San Cristóbal de La Laguna, Tenerife, Spain*
[5] *Instituto Universitario de Estudios Avanzados (IUdEA), Universidad de La Laguna, Apdo. 456, E-38200 San Cristóbal de La Laguna, Tenerife, Spain*
[6] *Laboratoire Hubert-Curien, UMR CNRS 5516, Université de Lyon, Université Jean Monnet, St. Etienne, F-42000 France*
**Corresponding author: guillermo.martin@univ-grenoble-alpes.fr*

Received XX Month XXXX; revised XX Month, XXXX; accepted XX Month XXXX; posted XX Month XXXX (Doc. ID XXXXX); published XX Month XXXX

Direct ultrafast laser photoinscription of transparent materials is a powerful technique for the development of embedded 3D photonics. This is particularly adapted for astrophotonic devices when multiple inputs are required. The process relies essentially on volume fabrication of waveguiding structures in flexible 3D designs and refractive index contrast parameters adjustable for specific spectral ranges. This enables 3D geometry and thus avoids in-plane crossings of waveguides that can induce losses and crosstalks in multi-telescope beam combiners. The additional novel capability of the technique allows for the fabrication of high aspect ratio nanostructures nonperturbatively sampling the optical field. Combining ultrafast laser micro and nanoprocessing with engineered beams, we present here results for the development of chip-sized silica glass integrated robust 3D three telescope beam combiners in the near infrared range, as well as embedded diffraction gratings, for phase closure analysis and spectro-interferometry applications in astronomy. © 2023 Optica Publishing Group

It is well known that the integrated optics beam combiner is considered as a good approach to reduce problems of stability, weight and compactness of interferometric instruments by packing several optical functions in one monolithic chip. Moreover, the use of single mode optical waveguides improves the modal filtering which is a compulsory step for increasing fringe contrast in high contrast interferometry applications. The astronomical goal is to combine the beams collected from different telescopes and study the interference fringes at different spectral channels [1, 2]. Therefore, development of miniaturized 3D IR spectro-interferometers that can be easily cooled down, are mechanically stable and have small footprint is very promising in particular for spatial applications. Among the different techniques available for waveguide fabrication, there has been a growing interest in ultrafast laser inscription (ULI) of waveguides using ultrashort femtosecond laser pulses and nonlinear excitation with high 3D spatial localization [3]. With this technique, optical confined structures are obtained by locally changing material properties such as the refractive index. Initial developments [4-11] confirmed ULI as a versatile tool for modifying the refractive index arbitrarily in X,Y,Z directions. In particular, in-plane X-crossing of waveguides is avoided, reducing crosstalk and increasing the compactness of the device. Thus, in the context of multi-telescope interferometry, it becomes possible to conceive and fabricate complex beam combiners of limited dimension. Additionally, the strong confinement associated with ultrashort optical pulses and beam engineering in one-dimensional geometries allows for in-chip processing of nanoscale diffractive structures [10].

In this paper we present the fabrication and characterization of a full miniaturized 3D near-IR spectro-interferometer using ULI, combining in the same chip the waveguides, beam combiners and diffraction grating, opening the way for compact spectro-interferometry.

1. 3D THREE TELESCOPES BEAM COMBINER

The device described here is a 3D-3T beam combiner that could be used in astronomy for phase closure studies [12-15]. The optical design was realized on a standard SiO_2 glass chip (Corning 7980) of

20x10x3 mm^3 size. An ultrafast laser inscription (ULI) technique employing 1030 nm 180 fs ultrashort laser pulses was applied in conditions similar to the one described in [8] with spatially-engineered beams adapted to the process. The waveguiding parts were realized using a transverse slit-shaping scan method [16] at 100 kHz and 0.3 mm/s scan speed. The soft interaction regime generates a positive index region with a refractive index contrast in the range of $2\text{-}3x10^{-3}$ measured at 632 nm wavelength and an estimated dimension of 8.5-10.5 μm waveguide core diameter. The laser written waveguides designed here are optimized for single mode behavior in the near-IR wavelength range (1.55 μm), with expected propagation losses below 1 dB/cm for straight guides [4]. The 3D-3T waveguide architecture design is shown in Figure 1, with a description of the laser-fabricated parts. The same ULI setup enables the generation of adapted beams for one-dimensional nanoscale structuring, which innovatively combines temporal pulse shaping and non-diffractive beam spatial engineering. This allows one to fabricate with high precision the embedded grating requested to sample the field over the whole waveguide array. The grating consists of 3 μm periodically spaced high aspect ratio void structures, with a cross-section diameter around 150 nm, photoinscribed transversally in the vicinity of the waveguides. These nanostructures are small enough not to perturb the traveling light modes in the waveguide, but they are able to extract a part of their evanescent field in a transverse scattering radiation, and then be focused onto a detector. The high aspect ratio nanostructures are obtained by engineering the laser beam via an axicon into non-diffracting Bessel beams of 9.7° half cone angle, with 50 μJ, 1kHz, 2 ps laser pulses at 1030 nm central wavelength [17]. The use of non-diffractive beams offers increased nonlinear stability and robustness against aberrations. The one-step fabrication of an "in-phase" grating covering simultaneously all the waveguides ensures that diffraction angle will be the same for all the waveguides (as opposed to fabricating one grating per waveguide that will present slight variations in period and therefore different diffraction angles). Finally, the choice of pre-chirped ps pulses favorizes the generation of voids, providing maximal coupling to the grating. This design allows to obtain in a single device the combination of optical signals coming from three different telescopes and an integrated signal extraction function using the ULI grating written close to the output of the combiner. As depicted in Fig. 1, three signals coming from their respective telescope are coupled into their respective input waveguide. They are secondly divided into two waveguides after a Y-junction. Thirdly, pairwise combinations are made with a second inverse Y-junction. By external scan of the relative optical phase delay (OPD) between the inputs, different interferograms are obtained in each output simultaneously. In classical instruments, the outputs are spectrally dispersed along the propagation axis. Here, information from the evanescent field of the waveguide is extracted and transversally radiated through an appropriate relay optics on the top of the sample surface, allowing us to directly acquire the spectrum. The main advantage of the 3D design is that in-plane crossings are no longer needed. Vertical shifting of the channel waveguides after beam splitting can now be made, in order to achieve pairwise combination. In the present case, vertical offsets of +/-125 μm were implemented. Straight input/output sections of 1 mm were also used, to ensure filtering out high order modes.

In parallel and close to the 3T beam combiner, a single straight channel waveguide was written, using the same laser parameters, in order to perform transmission measurements at a wavelength of 1.55 μm. By comparing the measured power with and without the sample, for a straight waveguide and for the 3D 3T (including the grating) we obtain global insertion losses of 3.4 dB for the straight waveguide (45% transmission). After correction for Fresnel losses and mode mismatch between single mode ULI waveguide (8 μm) as compared to the injection PM Panda fiber of a V-groove (10.1 μm), we obtain 1.7 dB/cm propagation losses at 1.55 μm, close to our recent findings on fused silica ULI waveguides at 3.4 mid-IR range [18].

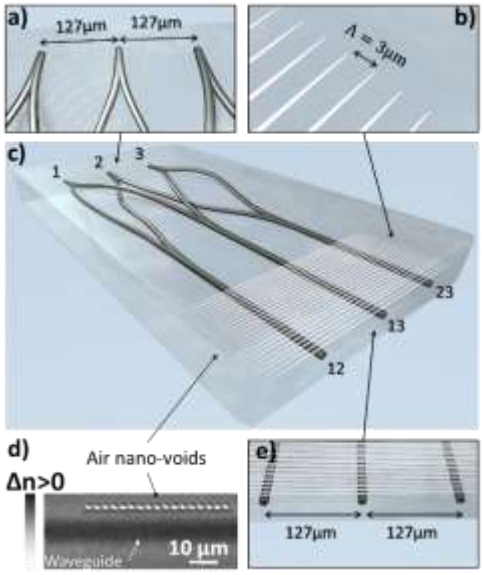

Fig. 1. Graphical representation of the device with: a) input a Y-splitters; b) periodic grating; c) concept of the 3D 3T beam combiner with embedded gratings; d) lateral microscopic view of the waveguide and the nanovoids and e) interferometric outputs with the grating on-top.

2. EXPERIMENTAL SET-UP FOR IMAGING GRATING DIFFRACTION

The experimental set-up is described in detail elsewhere [19, 20]. Simultaneous injection of the three inputs is done using PM fibers on a V-groove, and we can vary the relative optical path delay between the inputs and select the polarization state. Light diffracted by the grating is focused on an IR detector using a triplet of cylindrical lenses.

3. DIRECT SPECTRUM

The theoretical background of this spectrum mode [19, 20] is summarized here. The grating extracts light following the fundamental diffraction law; $n_{eff} + m\lambda/\Lambda = n_{bulk}\sin(\theta_1)$, where n_{eff} is the effective refractive index of the propagating mode, n_{bulk} the glass refractive index, Λ is the period of the grating, and m an integer giving the diffraction order and θ_1 the angle from the vertical direction. The theoretical resolution of the grating is given by $R = mL/\Lambda$, where respectively L and Λ are the length and the period of

the diffraction grating. As the relay optics and detector are perpendicular to the waveguide propagation axis, the diffracted order m is calculated using $\theta_1 = 0°$. For $\lambda = 1550$ nm and $\Lambda = 3$ μm, we obtain m = 3. Therefore, the theoretical spectral resolution, for L = 4 mm, is R = 4000. Experimentally, the spectral resolution is related to the pixel size, and therefore the ability to discriminate two close wavelengths. Besides, any inhomogeneity in the period of the nanovoids that form the grating will decrease the resolution, by increasing the width of the diffracted peak. To get an experimental value of the spectral resolution, a DFB laser light (bandwidth of 5 MHz) is injected and tuned (1548 nm < λ < 1553 nm) with a TEC controller. A first image of the diffracted signal extracted from the waveguides and focused on the detector thanks to the cylindrical triplet is shown in Fig. 2 (top).

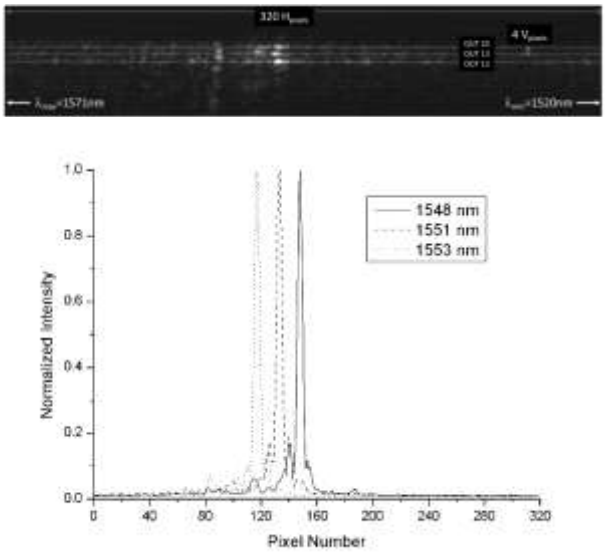

Fig. 2: Top: Diffracted peak obtained on the detector after monochromatic injection, showing the vertical separation for the three waveguides. The central area is saturated to observe the residual flux at other angles. Bottom: Intensity detected on the camera without saturation along the horizontal direction for waveguide OUT12, as a function of wavelength.

As shown in Fig. 2 (bottom), as the wavelength of the IR laser is modified, the peak moves accordingly along the horizontal line of pixels in the detector. From these measurements, we can extract the experimental resolution: 30 pixels corresponds to a wavelength variation of 5 nm, therefore 1 pixel = 5/30 = 0.16 nm. A peak width of 3.5 pixels (defined at an intensity corresponding to half of the intensity maximum) is measured. Therefore, our spectral resolution is defined as $R_{exp} = \lambda/\Delta\lambda$ = 1550 nm / (3.5x0.16 nm) = 2678 in good agreement with the theoretical value. This also allows us to get an idea of the wavelength bandwidth that can be analyzed with this system: The camera has 320 pixels laterally. As 30 pixels correspond to 5 nm, a wavelength range of around 51 nm is expected, with λ_{max} = 1571 nm on the left and λ_{min} = 1520 nm on the right, assuming aberrations won't enlarge the intensity peaks. Note however that the limiting factors for a large spectral bandwidth are the wavelength range in which the waveguides are single mode, and the spectral range before two different wavelengths at consecutive orders ($m\cdot\lambda_{max}$ and $(m+1)\cdot\lambda_{min}$) superimpose on the same pixel.

4. SPECTRO-INTERFEROMETER

After validation of the grating scattering, the second step is to introduce a time dependent optical delay between two inputs simultaneously injected, thanks to a translation stage in one of the input arms. In our case, signal is injected simultaneously in inputs 1 and 2, and therefore fringes are observed in output 12 ($OUT12_{FRG}$). As the signal injected in the input 3 is null, outputs 13 (OUT13) and 23 (OUT23) can be used as complementary photometric outputs. In Fig. 3 the optical responses of the device are shown for the horizontal polarization state (TE) following the OPD scanning. Note that the vertical (TM) polarization is several times weaker, as predicted by numerical calculations, and will not be studied (although it can be detected). This behavior can be explained by the fact that TM and TE polarizations correspond to mode electric field oscillations in the directions respectively parallel and perpendicular to the direction of the elongated Bessel structures, and have therefore anisotropic coupling with them. For this reason, the scattered intensity of the two polarization components is different and simulations are needed to understand the interaction efficiency as a function of groove size [21].

A. Monochromatic Scan

By scanning the relative OPD between inputs 1 and 2, the fringe evolution is obtained in Fig. 3. In this plot we correct the raw interference signal $OUT12_{FRG}$ with the true photometric outputs obtained by sequential measurement of OUT12 with only input 1 injected ($OUT12_1$), and then only input 2 ($OUT12_2$): $OUT12_{CORR} = 1 + (OUT12_{FRG} - OUT12_1 - OUT12_2)/(2\cdot\text{sqrt}(OUT12_1\cdot OUT12_2))$.

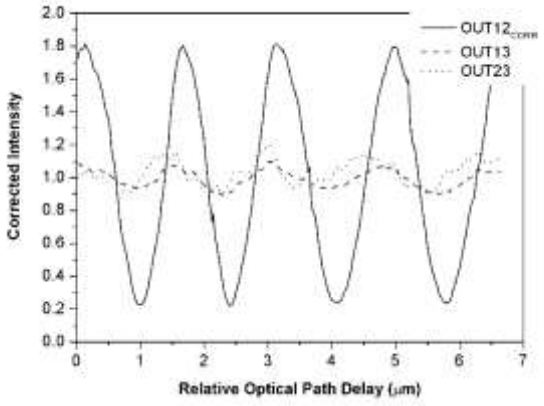

Fig. 3: Image of the monochromatic fringes of output peak 12 ($OUT12_{CORR}$), together with residual fringes observed in OUT13 and OUT23.

As shown in Fig. 3, the corrected data obtained for interferometric output 12 shows a good value of contrast (78%). However, low contrast oscillations can be observed in the central (OUT13) and upper (OUT23) waveguides, although no interferometric flux is expected. This can be an effect of stray light that could be reduced

using shifted inputs as in [10].

B. Polychromatic Scan

Using an ASE source (central emission at 1579 nm, 3 dB bandwidth of 90 nm), we can obtain the wideband response of the system. In Fig. 4 the diffracted intensity along the horizontal axis is observed, corresponding to different angles for different wavelengths. Here again, we initially set the system at OPD null position, where all the wavelengths have essentially the same phase.

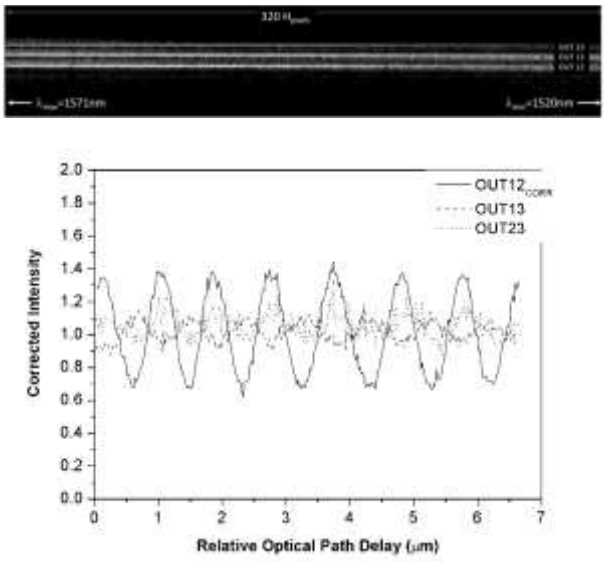

Fig. 4: Top: Image of the three waveguides as diffracted by the grating, in the wideband injection case. Bottom: OPD scan of the fringes around zero OPD using a wideband source.

As shown in the precedent figures, the diffracted signal from the waveguides can be studied in a window span of 55 nm, with a resolution around 2800, for a 4 mm long grating. The interference state of the fringes can thus be studied, as a function of wavelength, at different positions on the detector. Only three waveguides are considered and, as the imaging system gives a 1:1 image, only 4 pixels separate each waveguide vertically on the image. As 256 pixels are available on the vertical direction, there is enough space for increasing the number of waveguides and eventually increase the vertical separation of two adjacent waveguides. This would allow one to avoid optical overlapping between non interferometric channels and unexpected fringes appearing, in particular for monochromatic applications (see Fig. 3), and therefore increase fringe contrast. This can be useful for spectro-interferometry applications in astronomy using multi-T beam combiners such as in the FIRST/SUBARU project, where a minimum of 9 inputs is considered [22]. In this case, 3D design using ULI is probably the best option to reduce the chip length and avoid in-plane crossings, therefore reducing crosstalk and total losses.

5. CONCLUSIONS

Using an advanced laser photoinscription technique employing beam engineering, we have fabricated a 3D 3T spectro-interferometer useful for astronomical applications. The technique allows one to sample the signal efficiently with an innovative grating concept and reconstruct the spectral information. We have validated different technological parameters in order to develop single mode waveguides and high efficiency embedded gratings in silica glass in the near-IR. The obtained device shows good wide band contrast (>40% in average, for a source emitting at 1579nm and $\Delta\lambda$ = 90 nm) and satisfactory transmission losses (1.7 dB/cm).

Our next step will be to realize a complex device (typically 5 or more inputs) in order to prepare for next generation beam combiners, such as 6T VEGA/CHARA instruments, or the pupil remapper 5T FIRST/SUBARU, where some preliminary work has already been achieved [19]. As compared to FIRST instrument, for which R = 300, our compact spectro-interferometer should be an order of magnitude above. With this kind of 3D device we expect to address the problem of differential phase and high contrast interferometry, where a high number of beam combinations is needed, and avoiding in-plane crossings, crosstalk and stray light is compulsory.

Acknowledgments. Authors acknowledge the funding from ASHRA (Action Specifique Haute Resolution Angulaire) from INSU-CNRS and from the Agence Nationale de la Recherche via the project ANR2011 BS09 026 01 Smart_LasIR. A. Rodenas acknowledges "Fondo Social Europeo", "Fondo Europeo de Desarrollo Regional", "Agencia Canaria de Investigación Innovación y Sociedad de la Información" and "Agencia Estatal de Investigación" with project codes AEI/10.13039/501100011033, PRE2020-092762, PID2019-107335RA-I00, RYC-2017-21618, PROID2021010102 and EIS-2021-10, and also the European Innovation Council (EIC) Pathfinder reaCtor project under Grant Agreement 101099405.

Disclosures. The authors declare no conflicts of interest.

References

1. R. Abuter et al., Astron. Astrophys. **602**, 94 (2017).
2. D. Mourard et al., Astron. Astrophys., **508**, 2 (2009).
3. K. M. Davis, K. Miura, N. Sugimoto, and K. Hirao, Opt. Lett. **21**, 1729–1731 (1996).
4. S. Nolte, M. Will, J. Burghoff, and A. Tünnermann, Appl. Phys. A: Mater. Sci. Process. **77**, 109 (2003).
5. G. Della Valle, R. Osellame, P. Laporta, J. Opt. A **11**, 013001(2008).
6. A. Ródenas, G. Martin, B. Arezki, N. Psaila, G. Jose, A. Jha, L. Labadie, P. Kern, A. Kar, and R. Thomson, Optics Letters, Vol. **37**, 3, 392 (2012).
7. L. Labadie, G. Martin, N. C. Anheier, B. Arezki, H. A. Qiao, B. Bernacki, and P. Kern. Astron.Astrophys. **531**, A48 (2011).
8. G. Cheng, C. D'Amico, X. Liu, and R. Stoian. Opt. Lett. **38**, 1924 (2013).
9. S. Minardi. Mon. Not. R. Astron. Soc. **422**, 2656 (2012).
10. M. Bhuyan, P. K. Velpula, J. P. Colombier, T. Olivier, N. Faure, and R. Stoian. Appl. Phys. Lett. **104**, 021107 (2014).
11. N. Jovanovic, P. G. Tuthill, B. Norris, S. Gross, P. Stewart, N. Charles, S. Lacour, M. Ams, J. S. Lawrence, A. Lehmann, C. Niel, J. G. Robertson, G. D. Marshall, M. Ireland, A. Fuerbach and M. J. Withford, Mon. Not. R. Astron. Soc. **427**, 806–815 (2012).
12. D. Segransan, J.L. Beuzit, X. Delfosse, et al., Proc. SPIE **4006**, 269 (2000).
13. B. Lopez, R.G. Petrov, and M. Vannier, Proceedings of SPIE **4006**, 407 (2000).
14. M. Vannier, R.G. Petrov, B. Lopez, and F. Millour, MNRAS **367**, 825 (2006).
15. M. Zhao, J.D. Monnier, X. Che, et al., PASP **123**, 964 (2011).

16. Y. Cheng, K. Sugioka, K. Midorikawa, M. Masuda, K. Toyoda, M. Kawachi, and K. Shihoyama Opt. Lett. **28,** 55 (2003)
17. G. Zhang, G. Cheng, M. Bhuyan, C. D'Amico, and R. Stoian. Opt. Lett. **43**, 2161-2164 (2018).
18. Martínez, J., Ródenas, A., Fernandez, T., de Aldana, J. R. V., Thomson, R. R., Aguiló, M., Kar A. K., Solis J., and Díaz, F. Opt. Lett. **40**, 5818-5821 (2015).
19. G. Martin, M. Bhuyan, J. Troles, C. D'Amico, R. Stoian, and E. Le Coarer, Opt. Express **25**, 8386-8397 (2017).
20. G. Martin, F. Thomas, S. Heidmann, M. de Mengin, N. Courjal, G. Ulliac, A. Morand, P. Benech, P. Kern, E. Le Coarer. Proc. SPIE **9516**, 95160C (2015).
21. L. Arnaud, A. Bruyant, M. Renault, Y. Hadjar, R. Salas-Montiel, A. Apuzzo, G. Lérondel, A. Morand, P. Benech, E. Le Coarer, and S. Blaize, J. Opt. Soc. Am. A **30**, 2347-2355 (2013).
22. G. Martin, A. Morand, C. D'Amico, R. Stoian, K. Barjot, M. Lallement, N. Cvetojevic, S. Vievard, E. Huby, S. Lacour, V. Deo, O. Guyon, J. Lv, G. Zhang, G. Cheng. Proc. SPIE **12188**, 121882T (2022).

FULL LIST OF REFERENCES

1. R. Abuter et al., “First light for GRAVITY: Phase referencing optical interferometry for the Very Large Telescope Interferometer”, Astron. Astrophys. **602**, 94 (2017)
2. D. Mourard, J. M. Clausse, A. Marcotto, K. Perraut, I. Tallon-Bosc, Ph. Bério, A. Blazit, D. Bonneau, S. Bosio, Y. Bresson, O. Chesneau, O. Delaa, F. Hénault, Y. Hughes, S. Lagarde, G. Merlin, A. Roussel, A. Spang, Ph. Stee, M. Tallon, P. Antonelli, R. Foy, P. Kervella, R. Petrov, E. Thiebaut, F. Vakili, H. McAlister, T. ten Brummelaar, J. Sturmann, L. Sturmann, N. Turner, C. Farrington and P. J. Goldfinger “VEGA: Visible spEctroGraph and polArimeter for the CHARA array: principle and performance” Astron. & Astrophys., **508** 2, 1073-1083, (2009)
3. K. M. Davis, K. Miura, N. Sugimoto, and K. Hirao, “Writing waveguides in glass with a femtosecond laser,” Opt. Lett. **21**, 1729–1731 (1996).
4. S. Nolte, M. Will, J. Burghoff, and A. Tünnermann, “Femtosecond waveguide writing: a new avenue to three-dimensional integrated optics”Appl. Phys. A: Mater. Sci. Process. **77**, 109 2003.
5. G. Della Valle, R. Osellame, P. Laporta, “Micromachining of photonic devices by femtosecond laser pulses” J. Opt. A **11**, 013001(2008)
6. A.Ródenas, G. Martin, B. Arezki, N. Psaila, G. Jose, A. Jha, L. Labadie, P. Kern, A. Kar, and R. Thomson, “Three-dimensional mid-infrared photonic circuits in chalcogenide glass” Optics Letters, Vol. **37**, Issue 3, pp. 392-394 (2012).
7. L. Labadie, G. Martin, N. C. Anheier, B. Arezki, H. A. Qiao, B. Bernacki, and P. Kern. "First fringes with an integrated-optics beam combiner at 10 µm A new step towards instrument miniaturization for mid-infrared interferometry" Astronomy&Astrophysics **531**, A48 (2011).
8. G. Cheng, C. D’Amico, X. Liu, and R. Stoian. “Large mode area waveguides with polarization function by ultrafast laser photoinscription of a-SiO2”Opt. Lett. **38**, 1924 (2013).
9. S. Minardi. "Photonic lattices for astronomical interferometry" Mon. Not. R. Astron. Soc. **422**, 2656 (2012).
10. N. Jovanovic, P. G. Tuthill, B. Norris, S. Gross, P. Stewart, N. Charles, S. Lacour, M. Ams, J. S. Lawrence, A. Lehmann, C. Niel, J. G. Robertson, G. D. Marshall, M. Ireland, A. Fuerbach and M. J. Withford, “Starlight demonstration of the Dragonfly instrument: an integrated photonic pupil-remapping interferometer for high-contrast imaging” Mon. Not. R. Astron. Soc. **427**, 806–815 (2012)
11. M. Bhuyan, P. K. Velpula, J. P. Colombier, T. Olivier, N. Faure, and R. Stoian. “Single shot high aspect ratio bulk nanostructuring of fused silica using chirp controlled ultrafast laser Bessel beams” Appl. Phys. Lett. **104**, 021107 (2014)
12. D. Segransan, J.L. Beuzit, X. Delfosse, et al., "How AMBER will contribute to the search for brown dwarfs and extrasolar giant planets" Proceedings of SPIE **4006**, 269 (2000).
13. B. Lopez, R.G. Petrov, and M. Vannier, "Direct detection of hot extrasolar planets with the VLTI using differential interferometry", Proceedings of SPIE **4006**, 407 (2000).
14. M. Vannier, R.G. Petrov, B. Lopez, and F. Millour, MNRAS **367**, 825 (2006).
15. M. Zhao, J.D. Monnier, X. Che, et al., "Toward Direct Detection of Hot Jupiters with Precision Closure Phase: Calibration Studies and First Results from the CHARA Array"PASP **123**, 964 (2011).
16. Y. Cheng, K. Sugioka, K. Midorikawa, M. Masuda, K. Toyoda, M. Kawachi, and K. Shihoyama “Control of the cross-sectional shape of a hollow microchannel embedded in photostructurable glass by use of a femtosecond laser” Opt. Lett. **28,** 55 (2003)
17. G. Zhang, G. Cheng, M. Bhuyan, C. D’Amico, and R. Stoian. "Efficient point-by-point Bragg gratings fabricated in embedded laser-written silica waveguides using ultrafast Bessel beams,"Opt. Lett. **43**, 2161-2164 (2018)

18. Martínez, J., Ródenas, A., Fernandez, T., de Aldana, J. R. V., Thomson, R. R., Aguiló, M., Kar A. K., Solis J., and Díaz, F. “3D laser-written silica glass step-index high-contrast waveguides for the 3.5 μm mid-infrared range”. Optics Letters **40**, 5818-5821 (2015).
19. G. Martin, M. Bhuyan, J. Troles, C. D’Amico, R. Stoian, and E. Le Coarer, "Near infrared spectro-interferometer using femtosecond laser written GLS embedded waveguides and nano-scatterers," Opt. Express **25**, 8386-8397 (2017)
20. G. Martin, F. Thomas, S. Heidmann, M. de Mengin, N. Courjal, G. Ulliac, A. Morand, P. Benech, P. Kern, E. Le Coarer. “High Resolution TE&TM Near Infrared Compact Spectrometer based on Waveguide Grating Structures,” Proc. SPIE **9516**, 95160C (2015).
21. L. Arnaud, A. Bruyant, M. Renault, Y. Hadjar, R. Salas-Montiel, A. Apuzzo, G. Lérondel, A. Morand, P. Benech, E. Le Coarer, and S. Blaize, "Waveguide-coupled nanowire as an optical antenna," J. Opt. Soc. Am. A **30**, 2347-2355 (2013).
22. G. Martin, A. Morand, C. D'Amico, R. Stoian, K. Barjot, M. Lallement, N. Cvetojevic, S. Vievard, E. Huby, S. Lacour, V. Deo, O. Guyon, J. Lv, G. Zhang, G. Cheng. "FIRST 5T 3D: a laser written device for FIRST/SUBARU reducing crosstalk and propagation losses," Proc. SPIE **12188**, 121882T (2022).